

# Lessons learned using the insertable robotic effector platform (IREP) for single port access surgery

N. Simaan · A. Bajo · A. Reiter · Long Wang ·  
P. Allen · D. Fowler

Received: 28 January 2013 / Accepted: 18 March 2013 / Published online: 18 April 2013  
© Springer-Verlag London 2013

**Abstract** This paper presents the preliminary evaluation of a robotic system for single port access surgery. This system may be deployed through a 15-mm incision. It deploys two surgical arms and a third arm manipulating a stereo-vision module that tracks instrument location. The paper presents the design of the robot along with experiments demonstrating the capabilities of this robot. The evaluation includes use of tasks from fundamentals of laparoscopic surgery, evaluation of telemanipulation accuracy, knot tying, and vision tracking of tools.

**Keywords** Single port access surgery · Minimally invasive surgery · Natural orifice surgery

## Introduction

Single port access surgery (SPAS) is driven by the potential for added patient benefits due to reduction of the number of access incisions to only one (or to no incisions

when using a natural orifice). Compared to open or minimally invasive surgery (MIS), these potential benefits include improved cosmesis and patient self-image, reduced risk of wound site infection, and reduced pain. However, in order to deliver the potential patient benefits of SPAS over MIS, new technologies that address the technical demands of SPAS are needed. As an effort towards achieving this goal, our team has developed the Insertable Robotic Effector Platform (IREP), Fig. 1.

To enable SPAS, researchers investigated manual and robotic solutions. Examples of manual instruments include Realhand<sup>®</sup> from Novare, Cambridge Endo and Endo-SAMURAI from Olympus Corp., or Spider from Transenterix. These instruments provide distal tool tip dexterity and can articulate to avoid collisions between the operator hands [9]. Animal studies of single port access laparoscopic cholecystectomy have been reported using these instruments [8]. However, the use of manual instruments presents ergonomic challenges, requires surgeons to operate using un-intuitive hand movements and relies on exceptional hand–eye coordination and substantial training. More importantly, manual instruments do not harness the full potential of computer-aided surgery. Manual instruments only augment the surgeon's reach and dexterity. On the other hand, robotic systems are capable of augmenting sensory perception (e.g. by providing force sensing and feedback), interpretation of the surgical scene (e.g. by registering preoperative images to intraoperative scenes through the use of image overlay) and the accuracy and safety of surgical execution (e.g. by using active constraints or telemanipulation virtual fixtures).

For these reasons, researchers explored robotic assistance for SPAS and natural orifice transluminal endoscopic surgery (NOTES). Abbott [1] developed a wire-actuated dual-arm robotic system for NOTES which has 16 degrees

---

N. Simaan (✉) · A. Bajo · L. Wang  
A.R.M.A. Laboratory, Department of Mechanical Engineering,  
Vanderbilt University, Nashville, TN, USA  
e-mail: nabil.simaan@vanderbilt.edu

N. Simaan · A. Bajo · L. Wang  
Vanderbilt Initiative in Surgery and Engineering (VISE),  
Nashville, TN, USA

A. Reiter · P. Allen  
Department of Computer Science, Columbia University,  
New York City, NY, USA

D. Fowler  
Department of Surgery, Columbia University, New York City,  
NY, USA

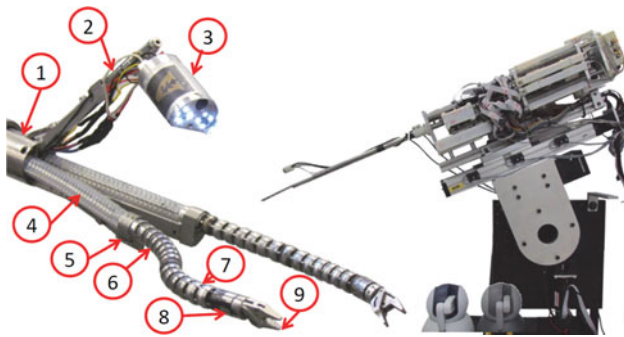


**Fig. 1** The IREP mounted on a rotational and a translational stage: (1) central stem, (2) three-DoF camera control arm, (3) vision module, (4) passively flexible stem, (5) parallelogram linkage, (6) first continuum segment, (7) second continuum segment, (8) rotational wrist, (9) gripper

of freedom (DoF) and a diameter ( $\varnothing$ ) larger than 20 mm. Kencana et al. [2] presented a 9 DoF  $\varnothing 22$  mm dual-arm robot. Lehman et al. [3] developed a NOTES robot that may be inserted into the abdomen via a  $\varnothing 20$  mm overtube and could be attached to the abdomen using external magnets. This design requires the surgeon to switch the device from a folded to a working configuration. Recently, Harada et al. [4] introduced a novel concept of a reconfigurable self-assembling robot for NOTES. This concept has yet to be experimentally proven. Lee et al. [5] presented a stackable four-bar mechanism for SPAS. Piccigallo et al. [6] presented a dual-arm robot for SPAS. This design embeds motors inside its surgical arms. Each arm is  $\varnothing 23$  mm and the requires access is  $\varnothing 30$  mm. Xu et al. [7] presented a concept for a trans-esophageal NOTES robot using design features of the IREP. Finally, Larkin et al. [8] presented a dual-arm SPAS system that uses wire-actuated snake-like articulated linkages. In contrast to this design, the IREP uses push–pull actuation and super-elastic NiTi backbones.

The IREP was designed by combining our past experience in designing systems for MIS of the throat [9] and for vision-guided automated surgical tool tracking [10]. The initial design considerations of this system have been described in [11, 12].

The IREP, we believe, is currently the smallest robotic system for SPAS, requiring an access port of only  $\varnothing 15$  mm while offering dual-arm dexterous operation with sub-millimeter accuracy, 3D visualization, and automated instrument tracking. It has two  $\varnothing 6.4$  mm dexterous surgical arms and a third arm manipulating a stereo-vision module. Each surgical arm includes a parallel mechanism, a passively flexible stem, an actively controlled continuum snake-like arm, a rotational wrist and a gripper. The parallel mechanisms control the distance between the bases of each snake arm. The total number of actuated DoF of the IREP is 21. These include seven actuated DoF for each

surgical arm, three DoF for deploying and controlling the pan/tilt of a vision module, two DoF for each gripper and two DoF for axial insertion of each dexterous arm.

The detailed kinematic modeling and design specifications of the IREP were presented in [13]. These specifications included the coverage of a workspace of at least 50 mm in each Cartesian direction, roll of the gripper about its longitudinal axis to enable suturing in confined spaces, ability to triangulate both surgical arms, ability to apply a 2-N lateral force in correspondence with surgical tissue manipulation forces and suturing [14], and  $\pm 0.25$  mm in positioning accuracy to allow micro-surgical interaction. The design avoids the use of serially connected motorized joints (such as in [15, 16]) in order to limit backlash and to enhance sterilizability. The IREP also provides a controllable distance between the bases of its dexterous surgical arms to increase kinematic dexterity and dual-arm triangulation. Ding et al. [12] showed these advantages compared to other designs using dexterous arms emanating from a single lumen (e.g. [17, 18]).

The IREP has also been designed as a modular platform for multi-modal use including energy and drug delivery and suction applications for SPAS and NOTES. This is achieved through the use of tubular access channels within each surgical arm. The flexible continuum arms can also be used as independent tools for NOTES by deploying them through an over-tube.

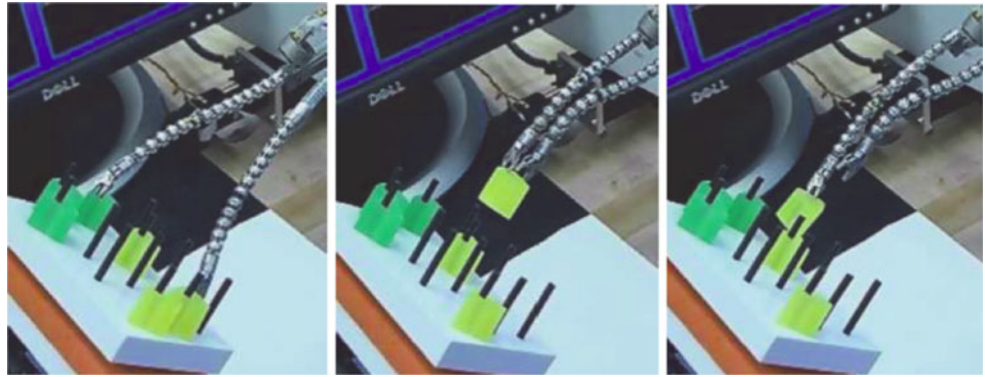
The following is a description of lessons learned during early evaluation experiments using the IREP.

## Materials and methods

To evaluate the IREP's functionality, we used several tasks including the Fundamentals of Laparoscopic Surgery (FLS) Manual Skills testing component (peg transfer and simple suture with intracorporeal knot). We also evaluated the accuracy of telemanipulation while following a circular path, tested the utility of our vision tracking algorithms and confirmed the workspace covered by a single arm against an adult life-size cholecystectomy trainer. Figure 2 shows the peg transfer experiment. Six rubber triangular parts with  $\varnothing 6.3$  mm holes were transferred from one side to the other side of a peg board with  $\varnothing 3.2$  mm pegs.

The IREP was tested in extreme conditions assuming that the only available gross movement of the device is along the trocar's longitudinal axis. We did not use all the four DoF available to standard MIS instruments since we wanted to determine the IREP's dexterity and workspace without reliance on these additional DoF. The peg transfer task consists of grasping a plastic ring with one hand, removing the ring from the peg, transferring the ring to the other hand, and then placing the ring on another peg

**Fig. 2** Dexterity peg board used for FLS evaluation



without dropping the ring. The simple suture and intracorporeal knot module consists of placing a suture through a dot on a rubber drain followed by tying intracorporeally a surgeon's knot and two square knots. Using these two modules, we could assess functionality of the robotic device under direct vision. If completed, we recorded the time to complete each module.

To evaluate telemanipulation accuracy and the effect of vision feedback using the IREP's cameras on user performance, we used a position-symmetric telemanipulation algorithm as described in [19]. A trained user was asked to move the robot's gripper along the circumference of a  $\varnothing 12$  mm circle. A grid paper with 500  $\mu\text{m}$  grid was used as a back-drop. A high-definition digital microscope was used to record a video of the robot movement and color-based image segmentation software was developed to locate the center of a printed red dot attached to the robot's gripper. This setup was needed since the movement accuracy of the IREP was very close or beyond the accuracy of commercial vision trackers available at our laboratory. Twenty experiments were equally split using two visual feedback methods: (a) using a high-definition microscope, (b) using the IREP's on-board cameras. We calculated the root mean square (RMS) and maximal tracking error and recorded completion times.

To demonstrate our tool tracking algorithm we overlaid the location of each gripper tracking box on the images of the vision module. We used vision tracking algorithms combining several different color and texture features in a probabilistic framework described in [20]. The features work together to assist each other when some cues are stronger than others, and the appearance of the tool is learned on-line. In this way, the tracker only requires an initial position and bounding box dimension on the first frame of the video sequence, and the appearance of the tool is learned on-the-fly as new views are presented to the camera and various conditions of the environment are changing. We have demonstrated this work in real surgical

scenarios [21] as well as with the IREP gripper in this paper.

Finally, we used a Simulab LC-10 cholecystectomy model. A surgeon telemanipulated one arm of the IREP to verify the extent of its reachable workspace. A sequence of experiment images was recorded.

## Results and discussion

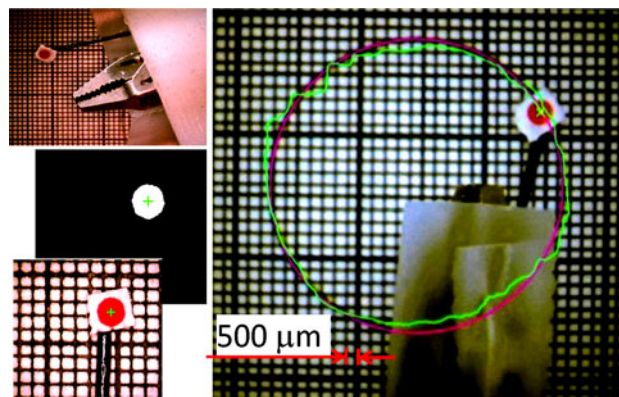
Figure 2 shows the results of the FLS experiment. The experiment validated that the grippers of the IREP were able to firmly hold the triangular objects, that the movement of the dexterous arms was sufficient to allow object transfer, and that each dexterous arm could cover the entire FLS peg board ( $64 \times 103$  mm). The experiment, however, did reveal that the telemanipulation code suffered from several flaws, including: (a) there was an unnecessarily high scaling ratio (5:1) between the master and slave, (b) coupling of motion between the master and slave was not direct, (c) rotation of the grippers about their axis slightly affected the gripper tip position, (d) although movement in the mid-range of the trocar's longitudinal insertion axis was intuitive for both hands, at the extremes of the range of movement in this axis the movement generated by the Cartesian stage carrying the IREP could only be controlled by the right master. Flaws (a–b) have later been fixed during debugging phases of the telemanipulation code. Flaw (c) is related to calibration of the continuum robotic arms and the fact that we used a Phantom Omni as the master interface, which made it difficult for the surgeon to rotate his hand in space without inducing translations. We have since then implemented an orientation telemanipulation mode. Exact calibration of the dexterous surgical arms remains a minor issue to address since our experience has shown that telemanipulation under surgeon vision allows for intuitive compensation for system imperfections.



Figure 3 shows the experiments in passing circular needles and knot tying. This experiment revealed that the limited roll of the gripper wrist made circular needle passing and hand exchange difficult. We initially designed the wrists to provide  $\pm 60^\circ$  of roll. This highlighted the need for a redesign of the distal wrist to provide a larger rotation workspace. To validate the amount of wrist roll we carried a straight needle at the gripper tip and rolled the wrist throughout its range of motion. By segmenting these images we determined that the manufactured wrist provided a roll range of  $\pm 69^\circ$ . Our new design goal is to provide at least  $360^\circ$  of roll. We have since then redesigned the wrists, but the new design has not been integrated yet.

Figure 4 shows a sample result of the telemanipulation experiment along the circumference of a  $\varnothing 12$  mm circle. The RMS and maximal tracking error along with the average experiment completion time are presented in Table 1. The maximal error was correlated with mechanical backlash in the actuation unit of the parallelogram linkage. These results informed the redesign of the actuation unit and we are setting up for repeating this experiment with multiple users.

Figure 5 shows successful tracking of the grippers using our probabilistic tracking framework. The red and blue boxes indicate the location of the gripper as detected by the tracking algorithm. The tracker was able to detect both grippers and to follow them successfully, but it was not



**Fig. 4** Visual tracking of the IREP's dexterous arms: (left) image segmentation of the gripper position, (right) the tracked trajectory against the desired movement trajectory

**Table 1** Results of the circle-following experiments

Vision source	RMS error (mm)	Max. error (mm)	Average time (s)
Microscope	0.24	1.2	47.6
IREP cameras	0.33	1.9	40.4

able to deal with scenarios where the gripper is temporarily hidden behind anatomy and then reappears in the image.

The cholecystectomy workspace verification experiment is shown in Fig. 6. We were successful in covering the

**Fig. 3** Visual tracking of the IREP's dexterous arms

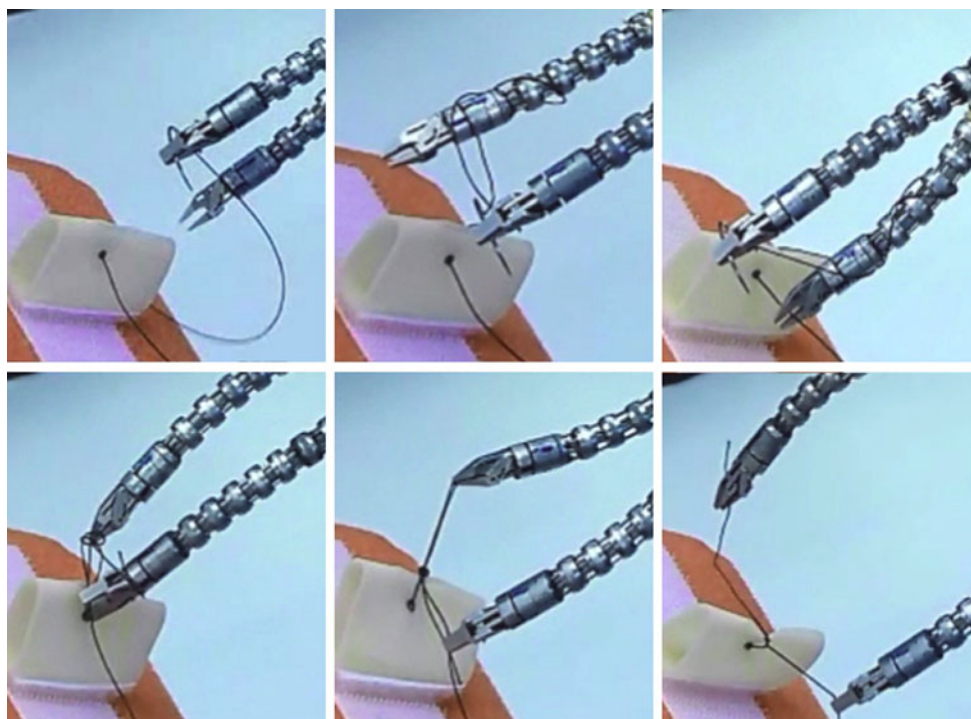
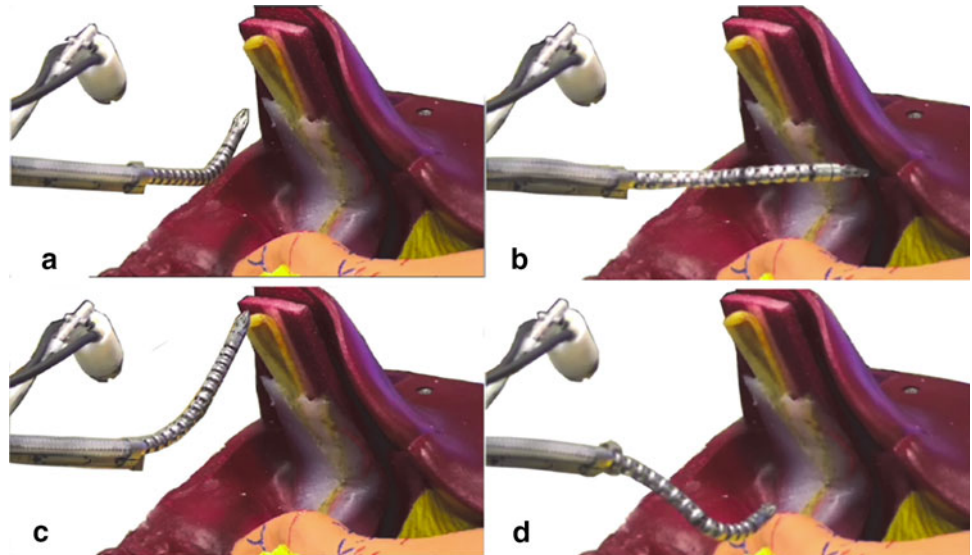


**Fig. 5** Visual tracking of the IREP's dexterous arms



**Fig. 6** Workspace boundaries of a single IREP arm shown against a cholecystectomy trainer: **a** left, **b** top, **c** right, **d** bottom



extends of an adult life-size model of a human gallbladder using only a single arm of the IREP, which agrees with our design goals as first stated in [11].

## Conclusion

We demonstrated that the IREP can complete object transfer, knot tying and automated vision tracking of its grippers. We also demonstrated that the workspace of a single arm of the IREP is suitable to cover the surgical field of cholecystectomy—even when the IREP is only mounted on an insertion slide and not all the traditional four DoF of MIS tools are used. This means that the IREP can be mounted on a simple support arm instead of a four-DoF robot. The evaluation also showed that the limited wrist roll complicated the passing of circular needles. We evaluated the actual roll range of the IREP and redesigned the wrist to provide at least one full turn. The telemanipulation experiments showed that the IREP is capable of sub-millimetric precision and that the  $640 \times 480$ -pixel cameras of the IREP degrade the user's performance. We are working

to incorporate higher resolution cameras. Evaluation of the IREP in the near future will include quantification of payload capabilities, telemanipulation latency, and evaluation on animals.

**Acknowledgments** This work was supported by NIH Grant No. 7R21EB007779. A. Bajo and N. Simaan were also supported by NSF Career Grant No. IIS-1063750. The evaluation experiments were performed under a research agreement with Titan Medical Inc. Dennis Fowler serves as a consultant for Titan Medical Inc.

**Conflict of interest** None.

## References

- Abbott DJ, Becke C, Rothstein RI, Peine WJ (2007) Design of an endoluminal NOTES robotic system. *IEEE/RSJ Int Conf Intell Robots Syst* 2007:410–416
- Kencana AP, Phee SJ, Low SC, Sun ZL, Huynh VA, Ho KY, Chung S (2008) Master and slave robotic system for natural orifice transluminal endoscopic surgery. *IEEE Conf Rob Autom Mechatron* 2008:296–300
- Lehman AC, Dumpert J, Wood NA, Visty AQ, Farritor SM, Oleynikov D (2008) In vivo robotics for natural orifice transgastric peritoneoscopy. *Stud Health Technol Inform* 132:236–241

4. Harada K, Susilo E, Menciassi A, Dario P (2009) Wireless reconfigurable modules for robotic endoluminal surgery. In: IEEE international conference on robotics and automation, 2009, pp 2699–2704
5. Lee H, Choi Y, Yi B-J (2010) Stackable 4-BAR manipulator for single port access surgery. *IEEE/ASME Trans Mechatron* 99:1–10
6. Piccigallo M, Scarfogliero U, Quaglia C, Petroni G, Valdastrì P, Menciassi A, Dario P (2010) Design of a novel bimanual robotic system for single-port laparoscopy. *IEEE/ASME Trans Mechatron* 15(6):871–878
7. Xu K, Zhao J, Geiger J, Shih AJ, Zheng M (2011) Design of an endoscopic stitching device for surgical obesity treatment using a N.O.T.E.S approach. In: IEEE/RSJ international conference on intelligent robots and systems, 2011, pp 961–966
8. Larkin DQ, Cooper TG, Duval EF, McGrogan A, Mohr CJ, Rosa DJ, Schena BM, Shafer DC, Williams MR (2007) Minimally invasive surgical system. U.S. Patent U.S. Patent 8182415 B22012
9. Simaan N, Xu K, Kapoor A, Kazanzides P, Flint P, Taylor R (2009) Design and integration of a telerobotic system for minimally invasive surgery of the throat. *Int J Rob Res* 28(9): 1134–1153
10. Hu T, Allen PK, Hogle NJ, Fowler DL (2009) Insertable surgical imaging device with pan, tilt, zoom, and lighting. *Int J Rob Res* 28(10):1373–1386
11. Xu K, Goldman R, Ding J, Allen P, Fowler D, Simaan N (2009) System design of an insertable robotic effector platform for single port access (SPA) surgery. In: IEEE/RSJ international conference on intelligent robots and systems, 2009, pp 5546–5552
12. Ding J, Goldman R, Allen P, Fowler D, Simaan N (2010) Design, simulation and evaluation of kinematic alternatives for insertable robotic effectors platforms in single port access surgery. In: IEEE international conference on intelligent robots and systems, 2010, pp 1053–1058
13. Ding J, Goldman RE, Xu K, Allen PK, Fowler DL, Simaan N (2012) Design and Coordination Kinematics of an insertable robotic effectors platform for single-port access surgery. *IEEE/ASME Trans Mechatron* 1–13
14. Dubrowski A, Sidhu R, Park J, Carnahan H (2005) Quantification of motion characteristics and forces applied to tissues during suturing. *Am J Surg* 190(1):131–136
15. Piccigallo M, Scarfogliero U, Quaglia C, Petroni G, Valdastrì P, Menciassi A, Dario P (2010) Design of a novel bimanual robotic system for single-port laparoscopy. *IEEE/ASME Trans Mechatron* 15(6):871–878
16. Lehman AC, Dumpert J, Wood NA, Visty AQ, Farritor SM, Oleynikov D (2008) In vivo robotics for natural orifice transgastric peritoneoscopy. *Stud Health Technol Inform* 132:236–241
17. Kencana AP, Phee SJ, Low SC, Sun ZL, Huynh VA, Ho KY, Chung S (2008) Master and slave robotic system for natural orifice transluminal endoscopic surgery. *IEEE Conf Rob Autom Mechatron* 2008:296–300
18. Abbott DJ, Becke C, Rothstein RI, Peine WJ (2007) Design of an endoluminal NOTES robotic system. *IEEE/RSJ Int Conf Intell Rob Syst* 2007:410–416
19. Bajo A, Goldman RE, Wang L, Fowler D, Simaan N (2012) Integration and preliminary evaluation of an insertable robotic effectors platform for single port access surgery. *IEEE Int Conf Rob Autom* 2012:3381–3387
20. Reiter A, Allen PK (2010) An online learning approach to in vivo tracking using synergistic features. *IEEE/RSJ Int Conf Intell Rob Syst* 2010:3441–3446
21. Hu T, Allen PK, Hogle NJ, Fowler DL (2009) Insertable surgical imaging device with pan, tilt, zoom, and lighting. *Int J Rob Res* 28(10):1373–1386